SLAC-PUB-10043
BABAR-TALK-02/104
July 2003

D^0 Mixing, Lifetime Differences, and Hadronic Decays of Charmed Hadrons

D.C.Williams[a] Representing the *BABAR* Collaboration

[a] Santa Cruz Institute of Particle Physics, University of California,
1156 High Street, Santa Cruz, CA 94040, USA

Presented are preliminary results from the *BABAR* Collaboration on charm physics, including limits on D^0 mixing from the ratio of lifetimes from $K^-\pi^+$, K^+K^-, and $\pi^+\pi^-$ final states (using 47.8 fb^{-1} of data) and branching ratio, and Dalitz amplitude analyses of the decays $D^0 \to K^0K^-\pi^+$, $\overline{K^0}K^+\pi^-$, and $\overline{K^0}K^+K^-$ (using 22 fb^{-1} of data). The status of direct measurements of D^0 mixing using wrong-sign $D^0 \to K^+\pi^-$ decays is also discussed.

1. INTRODUCTION

Because of a large charm cross section, e^+e^- colliders such as PEP-II that run near the $\Upsilon(4S)$ resonance produce copious amounts of charm hadrons. For example, there are approximately 120 million charm pair events contained in the current sample of 91 fb^{-1} data collected with the *BABAR* experiment. This data, currently the largest sample of charm available to any single experiment, is being used by the *BABAR* Collaboration for a series of charm studies.

Presented in this paper are summaries of two recent measurements: a limit on D^0 mixing from the ratio of lifetimes and Dalitz plot analyses of D^0 decays to K_S and two charged mesons. In addition, recently discovered issues involving the measurement of D^0 mixing using wrong-sign $K^+\pi^-$ decays are also discussed.

The *BABAR* detector, a general purpose, solenoidal, magnetic spectrometer, is described in more detail elsewhere [1].

2. D^0 MIXING

Like the K^0 and B^0 meson systems, D^0 mixing can occur if two D^0 states can be distinguished by either different widths Γ_1 and Γ_2 or different masses M_1 and M_2.[1] That is, if either of the quantities

$$x = \frac{1}{2}\frac{M_1 - M_2}{\Gamma_1 + \Gamma_2} \quad \text{or} \quad y = \frac{\Gamma_1 - \Gamma_2}{\Gamma_1 + \Gamma_2} \tag{1}$$

are non-zero, D^0 mesons will mix. Both x and y are expected to be small (10^{-3}) within the Standard Model [2]. A value of x whose magnitude $|x|$ is significantly larger than $|y|$ would be evidence of physics beyond the Standard Model.

2.1. Lifetime Ratios

The parameter y may be measured [3] using the D^0 lifetime $\tau_{K\pi}$ measured for a sample decaying into the Cabibbo-favored, *CP*-mixed $K^-\pi^+$ final state[2] and the lifetime τ_{hh} from a sample decaying into the Cabibbo-suppressed, *CP*-even K^-K^+ or $\pi^-\pi^+$ final states:

$$y = \frac{\tau_{K\pi}}{\tau_{hh}} - 1 \; . \tag{2}$$

Since all three of these final states have similar topologies, many systematic uncertainties in the D^0 lifetimes cancel in their ratio, making Eq. 2 a particularly sensitive measurement.

To identify D^0 candidates, pairs of oppositely charged tracks are combined in a fit which assumes a common point of origin. Charged K and π mesons are separated from other tracks using an algorithm that employs information from a

[1] The convention is that the parameters $\{\Gamma_1, M_1\}$ would be associated with the *CP*-even state if *CP* is conserved.

[2] In this paper, statements involving D^0 mesons and their decay modes are intended to apply in addition to their charged conjugates.

Work supported in part by the Department of Energy contract DE-AC03-76SF00515.

Stanford Linear Accelerator Center, Stanford University, Stanford, CA 94309
Presented at the 31st International Conference on High Energy Physics (ICHEP 2002),
Amsterdam, The Netherlands, 7/24/2002 - 7/31/2002

Cerenkov detector (DIRC) and dE/dx measured in the tracking chambers. The D^0 momentum p^* in the center-of-mass is required to be greater than 2.5 GeV/c^2 to remove contamination from B decays. To further reduce backgrounds, the D^0 is matched to a π^+ to form a D^{*+} candidate with a value of $\Delta m = m_{D^0} - m_{D^{*+}}$ within 2 to 3 MeV/c^2 of the peak, depending on the quality of π^+ track.

The lifetime of each D^0 sample is calculated using a unbinned maximum likelihood fit. The likelihood is divided into signal and background functions. The signal function is an exponential convoluted by a resolution function consisting of three Gaussians, the first two being proportional to the event-by-event decay time error and the third designed to catch outliers. The background distribution is similar, except that it includes a zero lifetime component. The probability that an event belongs to the signal is determined by comparing the reconstructed D^0 mass to a fit to the D^0 mass distribution. An example lifetime fit is shown in Fig. 1.

The values of y extracted from the lifetimes of the three D^0 samples are listed in Table 1 using 47.8 fb^{-1} of data collected during 2001–2002. Systematic uncertainties are calculated from the Monte Carlo by applying variations in event selection and event weights that correspond to the level of understanding of the detector response.

Table 1
Preliminary results for y. The first error is statistical; the second, systematic.

Decay	y (%)
$D^0 \to K^+K^-$	$1.6 \pm 1.2\ ^{+0.6}_{-0.7}$
$D^0 \to \pi^+\pi^-$	$1.0 \pm 1.7\ ^{+1.2}_{-1.4}$
Combined	$1.4 \pm 1.0\ ^{+0.6}_{-0.7}$

2.2. Wrong Sign $K^+\pi^-$ Decays

The selection of wrong-sign $D^0 \to K^+\pi^-$ decays is similar to the method described in the previous section. The Δm distribution of the resulting sample is shown in Fig. 2 and consists of approximately 600 signal events.

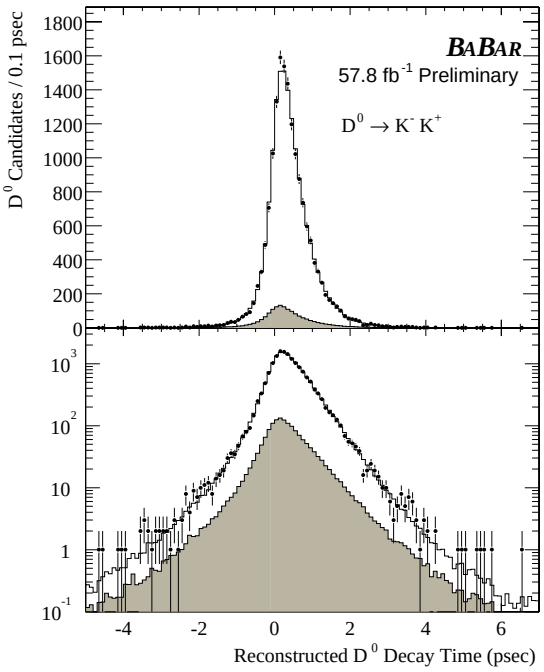

Figure 1. The fit to the reconstructed D^0 lifetime for the K^-K^+ decay mode for all events including the D^0 mass sidebands. The white histogram represents the result of the unbinned maximum likelihood fit described in the text. The gray histogram is the portion assigned to the background.

If CP is violated, the decay time distribution for D^0 mesons does not need to match that of their anti-particles $\overline{D^0}$. Each of these time distributions depend upon the parameters $|x'^{\pm}|$ and $y'^{\pm}$ [4]:

$$|x'^{\pm}| = |a_M\,(x'\cos\varphi y' \pm \sin\varphi)| \quad (3)$$

$$y'^{\pm} = a_M\,(y'\cos\varphi \mp x'\sin\varphi)\ , \quad (4)$$

where the upper (lower) sign corresponds to D^0 ($\overline{D^0}$) mesons, $\{x', y'\}$ are the mixing parameters $\{x, y\}$ rotated by an unknown strong phase, and $a_m = 1$ and $\varphi = 0$ in the limit of CP conservation. It has recently been recognized that, as a consequence of Eqs. 3 and 4, there is an eight-fold ambiguity in the values of $\{x', y', \varphi\}$. In particu-

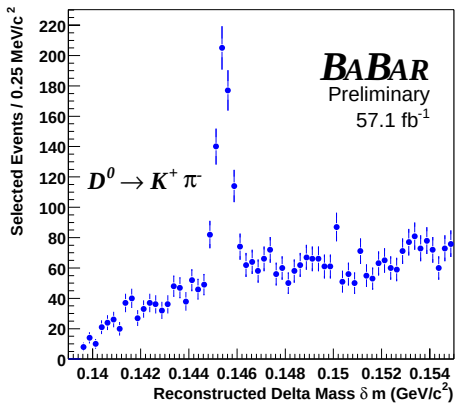

Figure 2. The Δm distribution of the $D^0 \to K^+\pi^-$ (wrong-sign) sample.

lar, the existence of one ambiguity $\{x', -y', \varphi+\pi\}$ prevents the measurement of the sign of y'.

3. THREE BODY D^0 DECAYS

The Dalitz plot analysis is the most complete method of studying the dynamics of three-body charm decays. Some of the cleanest such samples are those involving a K_S and two charged mesons: $D^0 \to K_S h^+ h^-$, where h is either a pion or kaon.

To identify these D^0 decays, K_S candidates are selected by combining all positive and negative tracks. False K_S candidates are removed by requiring a flight distance of at least 0.4 cm. Particle identification is used to select a clean sample of K^+ candidates. A D^* tag with a value of Δm within 2σ of the peak is used to remove background and distinguish between D^0 and $\overline{D^0}$.

The selection efficiencies for the four D^0 decay modes are determined by a sample of Monte Carlo events in which each decay mode is generated according to uniform phase space (such that the Dalitz plot is uniformly populated). The Dalitz distribution of events selected from these samples are used to calculate the acceptance of each event in the data. Background levels are estimated by fitting the D^0 mass distribution to a Gaussian on top of a linear background. Listed in Table 2 are the resulting branching ratios, based on a data sample of 22 fb^{-1} of data collected during 2001.

Table 2
Branching ratios relative to $D^0 \to \overline{K^0}\pi^+\pi^-$. The first error is statistical; the second, systematic. All numbers are preliminary.

Channel	Branching Ratio (%)
$D^0 \to K^0 K^-\pi^+$	$8.32 \pm 0.29 \pm 0.56$
$D^0 \to \overline{K^0} K^+\pi^-$	$5.68 \pm 0.25 \pm 0.41$
$D^0 \to \overline{K^0} K^- K^+$	$16.30 \pm 0.37 \pm 0.27$

An unbinned maximum likelihood fit is applied to the Dalitz distribution of $D^0 \to K^0 K^-\pi^+$, $\overline{K^0}K^+\pi^-$, and $\overline{K^0}K^+K^-$ in order to determine the relative amplitudes and phases of intermediate resonant and nonresonant (NR) states. Using a method employed by ARGUS [5] and CLEO [6], each resonant state is represented by an amplitude that is a product of a complex Breit-Wigner function and an angular function. The likelihood function consists of the sum of these amplitudes, normalized by the selection efficiency, and with a separate term for a flat contribution from background, the relative size of which is determined by the sidebands in a fit to the D^0 mass distribution.

The parameters of the resonant states are held fixed in the fit, with the exception of the width of the $\phi(1020)$ meson which is allowed to vary in order to approximately account for detector resolution. The $f_0(980)$ and $a_0(980)$ are described using coupled-channel Breit-Wigner functions with parameters taken from the CERN/WA76 [7] and the Crystal Barrel [8] experiments, respectively. The parameters of the $K_0^*(1430)$ ($m = 1.435$ GeV/c^2, $\Gamma = 279$ GeV/c^2) are taken from a recent reanalysis of LASS data [9]. The NR contribution is represented by a constant term.

The fraction and relative phase ϕ of each contribution to the fits are listed in Tables 3–5. The Dalitz plots and their projections are shown in Fig. 3. Systematic errors in the fractions are evaluated by varying the assumptions in the fits including removing the Blatt-Weisskopf terms and assuming a uniform acceptance.

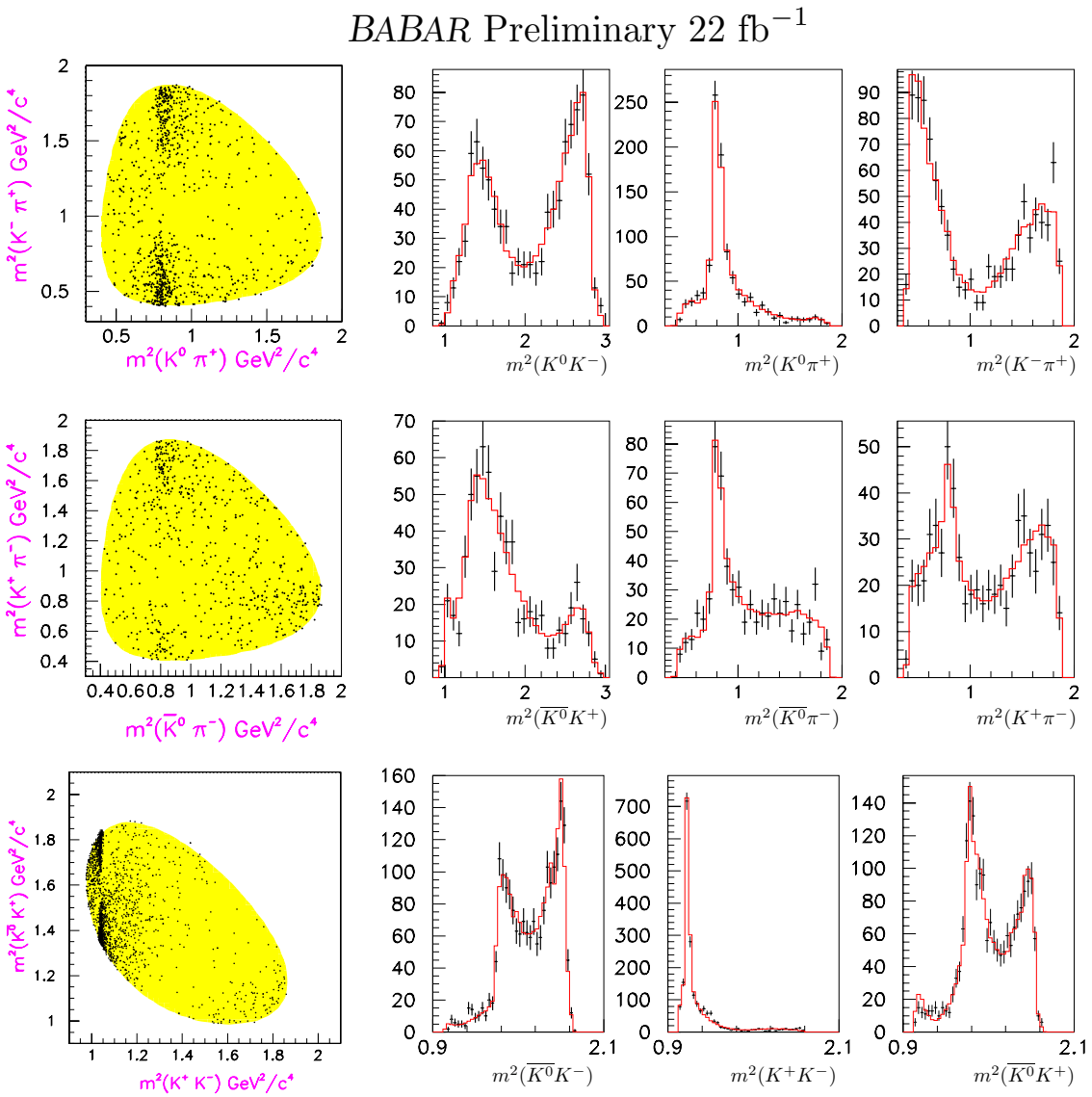

Figure 3. Dalitz plots and projections for (top row) $D^0 \to K^0 K^- \pi^+$, (middle row) $D^0 \to \overline{K^0} K^+ \pi^-$, and (bottom row) $D^0 \to \overline{K^0} K^+ K^-$. On the left are the Dalitz plots, with the kinematic region indicated in yellow. On the right are the three m^2 projections for (points) data and (histogram) the Dalitz plot fit.

Table 3
Preliminary results from the Dalitz plot analysis of $D^0 \to K^0 K^- \pi^+$. The first error is statistical; the second, systematic.

Final state	Fraction (%)	ϕ (degrees)
$\overline{K_0^{*0}}(1430)\ K^0$	$4.8 \pm 1.4 \pm 1.6$	52 ± 27
$\overline{K_1^{*0}}(892)\ K^0$	$0.8 \pm 0.5 \pm 0.1$	175 ± 22
$\overline{K_1^{*0}}(1680)\ K^0$	$6.9 \pm 1.2 \pm 1.0$	-169 ± 16
$\overline{K_2^{*0}}(1430)\ K^0$	$2.0 \pm 0.6 \pm 0.1$	51 ± 18
$K_0^{*+}(1430)\ K^-$	$13.3 \pm 3.5 \pm 3.9$	-41 ± 25
$K_1^{*+}(892)\ K^-$	$63.6 \pm 5.1 \pm 2.6$	0
$K_1^{*+}(1680)\ K^-$	$15.6 \pm 3.0 \pm 1.4$	-178 ± 10
$K_2^{*+}(1430)\ K^-$	$13.8 \pm 2.6 \pm 7.9$	-52 ± 7
$a_0^-(980)\ \pi^+$	$2.9 \pm 2.3 \pm 0.7$	-100 ± 13
$a_0^-(1450)\ \pi^+$	$3.1 \pm 1.9 \pm 0.9$	31 ± 16
$a_2^-(1310)\ \pi^+$	$0.7 \pm 0.4 \pm 0.1$	-149 ± 27
NR	$2.3 \pm 0.5 \pm 5.6$	-136 ± 23
Sum	130 ± 8	

Table 4
Preliminary results from the Dalitz plot analysis of $D^0 \to \overline{K^0} K^+ \pi^-$. The first error is statistical; the second, systematic.

Final state	Fraction (%)	ϕ (degrees)
$K_0^{*0}(1430)\ \overline{K^0}$	$26.0 \pm 16.1 \pm 3.3$	-38 ± 22
$K_1^{*0}(892)\ \overline{K^0}$	$2.8 \pm 1.4 \pm 0.5$	-126 ± 19
$K_1^{*0}(1680)\ \overline{K^0}$	$15.2 \pm 11.9 \pm 0.5$	161 ± 9
$K_2^{*0}(1430)\ \overline{K^0}$	$1.7 \pm 2.5 \pm 0.2$	53 ± 38
$K_0^{*-}(1430)\ K^+$	$2.4 \pm 8.2 \pm 1.0$	-142 ± 115
$K_1^{*-}(892)\ K^+$	$35.6 \pm 7.7 \pm 2.3$	0
$K_1^{*-}(1680)\ K^+$	$5.1 \pm 5.7 \pm 1.1$	124 ± 27
$K_2^{*-}(1430)\ K^+$	$1.0 \pm 1.0 \pm 0.2$	-26 ± 38
$a_0^+(980)\ \pi^-$	$15.1 \pm 12.5 \pm 0.6$	-160 ± 42
$a_0^+(1450)\ \pi^-$	$2.2 \pm 2.7 \pm 1.2$	148 ± 25
NR	$36.6 \pm 25.8 \pm 2.7$	-172 ± 13
Sum	144 ± 37	

ACKNOWLEDGEMENTS

We are grateful for the excellent luminosity and machine conditions provided by our PEP-II colleagues. This work is supported by DOE and NSF (USA), NSERC (Canada), IHEP (China), CEA and CNRS-IN2P3 (France), BMBF (Germany), INFN (Italy), NFR (Norway), MIST (Russia), and PPARC (United Kingdom). Individuals have received support from the Swiss NSF, A. P. Sloan Foundation, Research Corporation, and Alexander von Humboldt Foundation.

REFERENCES

1. The *BABAR* Collaboration, B. Aubert *et al.*, Nucl. Instr. Methods **A479** (2002) 1.
2. F. Buccella, M. Lusignoli, and A. Publiese, Phys. Lett. **B379** (1996) 249; F. Buccella *et al.*, Phys. Rev. **D51** (1995) 3478.
3. E. Golowich and S. Pakvasa, Phys. Lett. **B505** (2001) 94.
4. K. Hagiwara *et al.*, Phys. Rev. **D66** (2002) 010001.
5. H. Albrecht *et al.*, Phys. Lett. **B308** (1993) 435.
6. S. Kopp *et al.*, Phys. Rev. **D63** (2001) 092011.
7. T.A. Armstrong *et al.*, Z. Phys. **C51** (1991) 351.
8. A. Abele *et al.*, Phys. Rev. **D57** (1998) 3860.
9. D. Aston *et al.*, Nucl. Phys. **B296** (1998) 493. D. Aston and B. Dunwoodie, private communication.

Table 5
Preliminary results from the Dalitz plot analysis of $D^0 \to \overline{K}^0 K^+ K^-$. The first error is statistical; the second, systematic.

Final state	Fraction(%)	ϕ (degrees)
$\overline{K^0}\ \phi$	$45.4 \pm 1.6 \pm 1.0$	0
$\overline{K^0}\ a_0^0(980)$	$60.9 \pm 7.5 \pm 13.3$	109 ± 5
$\overline{K^0}\ f_0(980)$	$12.2 \pm 3.1 \pm 8.6$	-161 ± 14
$a_0(980)^+\ K^-$	$34.3 \pm 3.2 \pm 6.8$	-53 ± 4
$a_0(980)^-\ K^+$	$3.2 \pm 1.9 \pm 0.5$	-13 ± 15
NR	$0.4 \pm 0.3 \pm 0.8$	40 ± 44
Sum	155 ± 9	